Journal of Hepatocellular Carcinoma

Dovepress
open access to scientific and medical research

Open Access Full Text Article

ORIGINAL RESEARCH

LncRNA MEG3 Inhibits Tumor Progression by Modulating Macrophage Phenotypic Polarization via miR-145-5p/DAB2 Axis in Hepatocellular Carcinoma

Qing Wei[1,*], Guoman Liu[1,*], Zihua Huang[1,*], Yanyan Huang[1], Lizheng Huang[1], Zheng Huang[1], Xianjian Wu[2], Huamei Wei[3], Jian Pu[2]

[1]Graduate College of Youjiang Medical University for Nationalities, Baise, Guangxi, 533099, People's Republic of China; [2]Department of Hepatobiliary Surgery, Affiliated Hospital of Youjiang Medical University for Nationalities, Baise, Guangxi, 533000, People's Republic of China; [3]Department of Pathology, Affiliated Hospital of Youjiang Medical University for Nationalities, Baise, Guangxi, 533000, People's Republic of China

*These authors contributed equally to this work

Correspondence: Jian Pu, Affiliated Hospital of Youjiang Medical University for Nationalities, No. 18 Zhongshan two Road, Baise, Guangxi, 533000, People's Republic of China, Tel +86 776-2836646, Email Pujianym@163.com

Background: Hepatocellular carcinoma (HCC) is the predominant histological type of primary liver cancer, which ranks sixth among the most common human tumors. Tumor-associated macrophages (TAMs) are an important component of tumor microenvironment (TME) and the M2 macrophage polarization substantially contributes to tumor growth and metastasis. Long non-coding RNA (lncRNA) MEG3 was reported to restrain HCC development. However, whether MEG3 regulates macrophage phenotypic polarization in HCC remains unclear.

Methods: Bone marrow derived macrophages (BMDMs) were treated with LPS/IFNγ and IL4/IL13 to induce the M1 and M2 macrophage polarization, respectively. M2-polarized BMDMs were simultaneously transfected with adenovirus vector overexpressing MEG3 (Adv-MEG3). Subsequently, M2-polarized BMDMs were cultured for 24 h with serum-free medium, the supernatants of which were harvested as conditioned medium (CM). HCC cell line Huh7 was cultured with CM for 24 h. $F4/80^{+}CD68^{+}$ and $F4/80^{+}CD206^{+}$ cell percentages in M1-and M2-polarized BMDMs were calculated using flow cytometry. Huh7 cell migration, invasion and angiogenesis were determined via Transwell assay and tube formation experiment. Nude mice were implanted with Huh7 cells and Adv-MEG3-transfected M2-polarizd BMDMs, and tumor growth and M2 macrophage polarization markers were assessed. The binding between miR-145-5p and MEG3 or disabled-2 (DAB2) was verified by luciferase reporter assay.

Results: MEG3 presented lower expression in HCC tissues than in normal controls, and low expression of MEG3 was correlated to poorer prognosis of HCC patients. MEG3 expression was enhanced during LPS/IFNγ-induced M1 polarization, but was reduced during IL4/IL13-induced M2 polarization. MEG3 overexpression inhibited the expression of M2 polarization markers in both M2-polarized BMDMs and mice. Mechanically, MEG3 bound with miR-145-5p to regulate DAB2 expression. Overexpressing MEG3 suppressed M2 polarization-induced HCC cell metastasis and angiogenesis by upregulating DAB2 and inhibited in vivo tumor growth.

Conclusion: LncRNA MEG3 curbs HCC development by repressing M2 macrophage polarization via miR-145-5p/DAB2 axis.

Keywords: hepatocellular carcinoma, tumor microenvironment, macrophage polarization, MEG3, miR-145-5p, DAB2, metastasis

Introduction

Primary liver cancer ranks sixth among the most common human tumors, making it a significant cause of a high fatality rate globally.[1] Hepatocellular carcinoma (HCC), which accounts for nearly 90% of primary liver cancer, is the predominant histological type.[2] HBV and HCV infections, excessive alcohol consumption, smoking, consumption of aflatoxin-contaminated food, liver fluke infections, and having diseases such as non-alcoholic steatohepatitis, obesity,

Received: 16 February 2023
Accepted: 26 June 2023
Published: 5 July 2023

type 2 diabetes and metabolic syndrome have all been identified to be the critical risk factors contributing to the occurrence of HCC.[3,4] In recent decades, continuous progresses have been achieved in HCC treatment methods including surgical resection, interventional therapy, immunotherapy, targeted therapy, radiotherapy, and chemotherapy, which have substantially improved survival in HCC patients and reduced global cancer burden.[5,6] Nevertheless, due to the high incidence of postoperative tumor recurrence and metastasis, the long-term prognosis for HCC patients remains poor.[7] In such a predicament, illuminating the molecular mechanisms underlying HCC development and identifying novel reliable biomarkers and therapeutic targets for HCC treatment are the prior tasks.

Tumor microenvironment (TME), which is composed of tumor cells, surrounding immune and inflammatory cells, tumor-associated fibroblasts, nearby mesenchymal tissue, microvasculature, and various cytokines and chemokines, is a complex comprehensive system.[8] Increasing studies have demonstrated that TME plays an essential role in tumor growth and metastasis, providing a crucial ecological niche for cancer initiation and progression.[9] Tumor-associated macrophages (TAMs) refer to macrophages infiltrated in tumor tissues and are an important component of TME.[10] Macrophages can be polarized into M1 or M2 phenotypes under different stimulations, showing their plasticity in response to environmental cues.[11] The polarization of macrophage is closely associated with tumorigenesis: M1-type macrophages are pro-inflammatory and promote tumoricidal responses while M2-type macrophages are anti-inflammatory facilitate tumor progression.[12] Multiple reports have elucidated that macrophages are involved in cancer development, including HCC, through regulating tumor cell growth, metastasis and angiogenesis in a polarized manner.[13,14] Macrophages are excellent candidates for cell therapy, and chimeric antigen receptor macrophages (CAR-M) are already in clinical evaluation.[15] Macrophage-targeted therapy is expected to be the next frontier in tumor immunotherapy.[16] Thus, it is crucial to elucidate the molecular mechanisms underlying the interaction between macrophage polarization and cell malignant phenotypes, which may provide novel therapeutic strategies for HCC.

Long non-coding RNAs (lncRNAs) are a class of regulatory transcripts longer that are 200 nucleotides or longer but have limited protein-coding potential.[17] It is well documented that lncRNAs are extensively involved in various pathophysiological processes through their multi-level regulation of gene expression and signal transduction.[18] Furthermore, massive studies have clarified that lncRNAs are frequently deregulated in human cancers and their abnormal expression and mutation are linked with cancer cell growth, apoptosis, cell cycle, senescence, differentiation, invasion, migration, drug resistance, and so on.[19,20] The role of lncRNAs is closely related to their cellular localization. LncRNAs in the nucleus mainly affect chromatin structure, chromatin remodeling, transcriptional regulation and nucleosome regulation, while lncRNAs in the cytoplasm affect mRNA stability, protein translation and post-translational modifications.[21] LncRNAs perform their biological functions through complex and various mechanisms, one of which is acting as microRNA (miRNA) sponges or competing endogenous RNAs (ceRNAs) to competitively bind to common miRNAs and relieve their repression on target genes.[22] Evidence has shown that numerous lncRNAs participate in HCC development at almost every stage.[23,24] LncRNA MEG3, which was initially found as a homologous imprinted gene of mouse GLT2, is located in the DLK1-MEG3 imprinting region of human chromosome 14.[25] Researchers have found that MEG3 is downregulated in multiple neoplasms including HCC, gastric cancer, prostate cancer, non-small cell lung cancer, cervical cancer, etc., and is regarded as a potential tumor suppressor.[26–29] Ectopic expression of MEG3 has been proved to suppress the growth and metastasis but enhance the apoptosis of tumor cells.[30] In contrast, deletion or low expression of MEG3 is largely related to early metastasis, deep infiltration, and low survival rate.[25] Even though MEG3 have been widely reported to inhibit HCC progression through regulating cancer cell malignant behaviors,[31] its role in macrophage polarization in HCC remains unclear until now.

In our study, the function of MEG3 on macrophage polarization during HCC development as well as the underlying molecular mechanisms were investigated. We hypothesized that MEG3 might restrain HCC cell metastasis and angiogenesis by curbing M2 macrophage phenotypic polarization through the MEG3/miR-145-5p/disabled-2 (DAB2) ceRNA regulatory network. Our study highlights the vital effects of lncRNA MEG3 in HCC progression and provides a feasible novel direction to identify therapeutic target for HCC.

Materials and Methods

Cell Culture and Treatment

Bone marrow derived macrophages (BMDMs) were isolated as described previously from C57BL/6 mice.[32,33] In brief, mouse femurs and tibias were removed using aseptic techniques and washed 2 to 3 times in a cell culture dish supplemented with PBS. By using syringes fit with 26-gauge needles, bone marrow cells were flushed into sterile tubes. Cells were incubated in complete Dulbecco's modified Eagle's medium (DMEM; Gibco, Invitrogen, Carlsbad, CA, USA) containing 10% fetal bovine serum (FBS; Gibco), 1% penicillin–streptomycin (Gibco) and 10 ng/mL macrophage colony-stimulating factor (M-CSF; PeproTech, Rocky Hill, NJ, USA) for 7 days at 37°C with 5% CO_2 to obtain BMDMs. To promote the differentiation of BMDMs into M1 or M2 macrophages, cells were treated for 48 h with 10 ng/mL LPS (Sigma-Aldrich, St. Louis, MO, USA)/IFNγ (eBioscience, San Diego, CA, USA) and 10 ng/mL IL4 (eBioscience)/IL13 (Sino Biological, China), respectively.[34] Subsequently, M2-polarized BMDMs were cultured for 24 h with serum-free medium, the supernatants of which were harvested as conditioned medium (CM) and were stored at −80°C. HCC cell line Huh7 was obtained from the Chinese Academy of Sciences Cell Bank and cultured in DMEM (Gibco). To explore the effects of M2 macrophage polarization on HCC cell phenotypes, Huh7 cells were cultured with CM obtained from M2-polarized BMDMs for 24 h.

Cell Transfection

To investigate the impacts of MEG3 overexpression on M2-polarization of BMDMs, MEG3 was inserted into the adenovirus vector to construct the recombinant overexpression vector (Adv-MEG3) by using AdenoBuilder toolkit (#1000000176; Addgene), with Adv-NC as the negative control. Recombinant adenovirus vector carrying a short hairpin RNA (sh-RNA) targeting DAB2 (Adv-shDAB2; top strand: 5'-CACCGGATAAAGAGATCAA GGATGTCGAAACATCCTTGATCTCTTTATCC-3', bottom strand: 5'-AAAAGGATAAAGAGATCAAGGATGT TTCGACATCCTTGATCTCTTTATCC-3') was generated to knockdown DAB2, with Adv-shNC (top strand: 5'-CACCGAGAGAAGAGGATATAATCGTCGAAACGATTATATCCTCTTCTCTC-3', bottom strand: 5'-AAAAGAGA GAAGAGGATATAATCGTTTCGACGATTATATCCTCTTCTCTC-3') as the negative control. MiR-145-5p mimics (5'-GUCCAGUUUUCCCAGGAAUCCCU-3') was used to overexpress miR-145-5p, with miR-NC (5'-GUCUAGAUCCUCAGCUCUGACCU-3') as the negative control. BMDMs or Huh7 cells were cultured in six-well plates and cell transfection was performed by using Lipofectamine 2000 (Invitrogen) after 80% confluence was reached. Transfection efficiency was examined 48 h post transfection by RT-qPCR.

Flow Cytometric Analysis

After 48 h of indicated treatment or transfection, 5×10^4 BMDMs were harvested and washed with PBS, followed by incubation with PE-conjugated anti-mouse CD86 antibody (ab275357, Abcam, Cambridge, UK), PE-conjugated anti-mouse CD206 (#141706, BioLegend, California, USA), or FITC-conjugated F4/80 (ab105155, Abcam) for 30 min. Data were analyzed with the help of a FACSCanto flow cytometer (BD biosciences).

Transwell Assay

The 24-well transwell chambers (8-μm pore size; Corning Costar, Tewksbury, MA, USA) were used to detect cell migration and invasion. A total of 3×10^4 Huh7 cells were resuspended in 200 μL serum-free medium and seeded into the upper chamber pre-coated with (for invasion assay) or without (for migration assay) Matrigel (Yeasen, Shanghai, China). Then, 600 μL complete culture medium was added to the bottom chamber. Plates were maintained in 5% CO_2 at 37°C for 24 h. Afterwards, cells that migrated or invaded the lower filter surfaces were fixed with 90% ethanol and stained with 0.1% crystal violet (Beyotime, Shanghai, China). Migrated or invaded cell numbers in five randomly selected fields of view were photographed with an IX81 microscope (Olympus) and quantified using Image-Pro Plus 6.0 software.

Tube Formation Assay

After indicated treatment or transfection, a total of 1×10^6 Huh7 cells were cultured in six-well plates for 48 h. The media were then harvested and used in the in vitro endothelial cell tube formation assay. In brief, the 96-well plates were pre-chilled on the ice. Subsequently, each well was added with 100 μL Matrigel and allowed to set for 30 min at 37°C. HUVECs were incubated with tumor-conditioned media for 8 h. Finally, the capillary-like structures were photographed.

Fluorescence in situ Hybridization (FISH) Assay

BMDMs were first stimulated by LPS/IFNγ and IL4/IL13 to induce M1 and M2 polarization, and were harvested after 24 or 48 h. Then, the M1- or M2-type BMDMs were fixed by 4% paraformaldehyde, washed by PBS, and permeabilized with 0.4% Triton X-100. Cells were prehybridized with a hybridization solution and then incubated with digoxigenin-labeled probe specific for MEG3, which was designed and synthesized by RiboBio (Guangzhou, China), in hybridization buffer. After overnight incubation in a humidified atmosphere at 37°C, cells were washed thrice in the dark by SSC reagent. Cells were stained with 4, 6-diamidino-2-phenylindole (DAPI; Beyotime) in the dark for 10 min, washed thrice with PBS, and photographed by fluorescence microscopy (Olympus).

Western Blotting

Huh7 cells were lysed with RIPA buffer (Cowin Biotech, Beijing, China) containing protease and phosphatase inhibitors. Equal amounts of denatured protein were transferred to PVDF membrane (Millipore) after separation on SDS–PAGE gels. After blocking with 5% skim milk, the membrane was incubated overnight at 4°C with primary antibodies including anti-DAB2 (ab256524) and anti-GAPDH (ab181602) diluted in TBS containing 0.05% Tween 20 (TBST) containing 3% bovine serum albumin (BSA). The next day, the membranes were washed with TBST and then incubated with HRP-labeled secondary antibody (ab7090) at RT for 1 h. The enhanced chemiluminescence (ECL) method was adopted to visualize and detect the protein signals.

Luciferase Reporter Assay

Based on the manufacturer's protocols for the Dual-Luciferase Reporter Assay System (Promega, Madison, WI, USA), dual-luciferase reporter assay was performed to validate the binding between MEG3 (or DAB2) and miR-145-5p. Briefly, the fragments of MEG3 and DAB2 3′UTR containing the predicted binding sites of wild-type or mutant miR-145-5p were inserted into the pmirGLO plasmid (Supplementary Figure 1; Promega) using the one-step directed cloning kit (Novoprotein, Shanghai, China) to construct the luciferase reporter plasmids pmirGLO-MEG3-Wt/Mut (Supplementary Figures 2 and 3) and pmirGLO-DAB2 3'UTR-Wt/Mut (Supplementary Figures 4 and 5), respectively. Huh7 cells were co-transfected with pmirGLO-MEG3-Wt/Mut or pmirGLO-DAB2 3'UTR-Wt/Mut plasmids, together with miR-145-5p mimics or negative control miR-NC. Transient transfections were achieved by using FuGene HD Transfection Reagent (Promega). After 48 h, the luciferase activity was detected using the Dual-Luciferase Reporter Assay System (Promega, Madison, WI, USA) on a Glomax20/20 luminometer (Promega).

Nude Mouse Xenograft Model

The Animal Care and Use Committee of Affiliated Hospital of Youjiang Medical University for Nationalities (Ethic Number: YYFY-LL-2022-112) approved the procedures in our animal experiments. All animals were handled following the guidelines of the National Institutes of Health Guide for the Care and Use of Laboratory Animals (Bethesda, MD). A total of 24 male BALB/c nude mice (4–5 weeks old) purchased from Charles River (Beijing, China) were used. Mice were randomly separated into three groups (N = 8 in each group): Huh7 (mice were injected with Huh7 cells) group, Huh7 + M2-type BMDMs-Adv-NC (mice were injected with Huh7 cells and Adv-NC-transfected M2-type BMDMs) group, and Huh7 + M2-type BMDMs-Adv-MEG3 (mice were injected with Huh7 cells and Adv-MEG3-transfected M2-type BMDMs) group. The mixture of Huh7 cells (1×10^6) and Adv-NC or Adv-MEG3-transfected M2-type BMDMs (6×10^6) was planted into mice armpits subcutaneously.[34] Mice were sacrificed four weeks later and the primary tumors were excised, imaged and weighed.

RNA Extraction and Real-Time Quantitative Polymerase Chain Reaction

Total RNA from BMDMs, Huh7 cells or tumor tissues was extracted using TRIzol reagent (TaKaRa, Dalian, China). Reverse-transcription of 1 μg of RNA was conducted by employing HiScript III RT SuperMix (Vazyme, Nanjing, China) to obtain complementary DNA (cDNA). The cDNA was subjected to real-time PCR on a CFX Connect PCR system (Bio-Rad) by using the ChamQ SYBR qPCR Master Mix (Vazyme). GAPDH and U6 served as the internal controls. Relative gene expression was calculated using the $2^{-\Delta\Delta CT}$ method.

Histopathology Evaluation

Fresh tumor tissues of mice were fixed with 10% formaldehyde solution, dehydrated with ethanol of gradient concentrations and xylene, embedded in paraffin, and cut down into slices of 5 μm. After dewaxing, the sections were stained with hematoxylin and eosin (H&E), mounted with neutral gum, and observed under a light microscope (Leica Microsystems, Wetzlar, Germany) to examine histopathological changes.

Immunohistochemistry Staining

Tumor tissues were embedded in paraffin and then sliced into 5-μm-thick sections. Then, the slides were dewaxed in xylene, rehydrated with gradient alcohol, antigen retrieved in water bath, and blocked with goat serum. After overnight incubation at 4°C with anti-CD206 (K010042P; 1:100; Solarbio, Beijing, China) and anti-Ki67 (K010075P; 1:200; Solarbio) primary antibodies, the sections were further incubated with secondary antibody (K0034G-AP; 1:100; Solarbio) for 20 min, followed by color development using DAB detection kit (ZSGB-BIO, China). At last, sections were counterstained with hematoxylin, mounted under coverslips, and imaged using a Pannoramic MIDI slide scanner (3DHISTECH Ltd, Budapest, Hungary).

Statistical Analysis

All statistical analyses were accomplished by using GraphPad Prism 5.0. The data of three independent experiments are expressed as the mean ± standard deviation (SD). As for the comparison between two groups and among multiple groups, Student's two-tailed *t*-test and one-way analysis of variance were adopted, respectively. $p < 0.05$ was considered statistically significant.

Results

Low Expression of MEG3 Predicts Poor Prognosis in HCC Patients

According to GEPIA database, MEG3 presents lower expression in LIHC tissues than in normal tissues (Figure 1A). Survival analysis in Kaplan Meier Plotter database showed that HCC patients with low expression of MEG3 had shorter overall survival time than those with high expression of MEG3 (Figure 1B), indicating the direct correlation between MEG3 expression and poor prognosis in HCC.

MEG3 Participates in M1/M2 Macrophage Polarization

To investigate the role of MEG3 in macrophage polarization, BMDMs were first treated with 10 ng/mL LPS/IFNγ to induce M1 macrophage polarization. By using flow cytometry, we discovered that $F4/80^{+}CD68^{+}$ cell percentage was significantly increased after LPS/IFNγ treatment, suggesting the induction of M1 macrophage polarization (Figure 2A and B). LncRNA MEG3 expression in control BMDMs and LPS/IFNγ-treated BMDMs was then detected. RT-qPCR analysis showed that LPS/IFNγ treatment markedly enhanced the expression of MEG3 (Figure 2C). Similarly, to induce M2 macrophage polarization, BMDMs were stimulated by 10 ng/mL IL4/IL13. As revealed by flow cytometric analysis, IL4/IL13 stimulation resulted in a remarkable increase in $F4/80^{+}CD206^{+}$ cell percentage, indicating the successful induction of M2 macrophage polarization (Figure 2D and E). Compared to control BMDMs, IL4/IL13-treated BMDMs displayed lower expression of MEG3 (Figure 2F). In addition, FISH assay was performed to further confirm MEG3 expression in M1-type and M2-type macrophages. As shown in Figure 2G and H, MEG3 expression in LPS/IFNγ-induced M1-type BMDMs was elevated by LPS/IFNγ treatment in a time-dependent manner. However, IL4/IL13

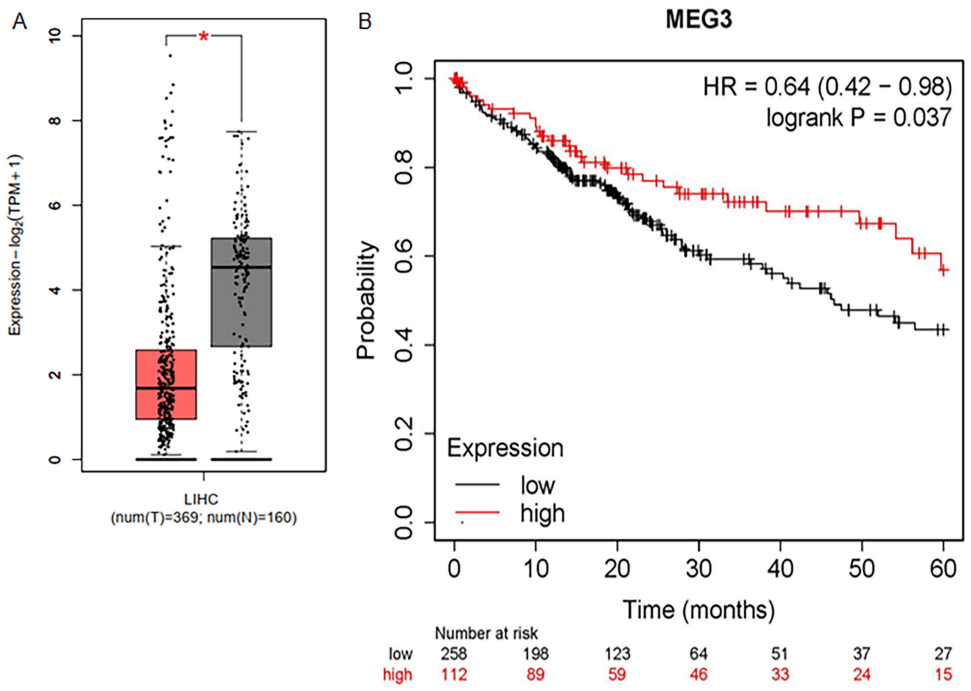

Figure 1 Low expression of MEG3 predicts poor prognosis in HCC patients. (**A**) The expression pattern of lncRNA MEG3 in 369 LIHC tissues and 160 normal tissues shown at GEPIA database (http://gepia.cancer-pku.cn/). (**B**) The overall survival time of HCC patients with high or low expression of MEG3 predicted at Kaplan Meier Plotter database (https://kmplot.com/analysis/). *p < 0.05.

treatment inhibited MEG3 expression in cytoplasm with a negative correlation with time growth in IL4/IL13-induced M2-type BMDMs (Figure 2I and J). Overall, MEG3 expression was altered during M1/M2 macrophage polarization.

MEG3 Suppresses M2 Macrophage Polarization

To figure out the detailed function of MEG3 in M2 macrophage polarization, we constructed adenovirus vector over-expressing MEG3 (Adv-MEG3) to promote MEG3 expression in M2-type BMDMs. RT-qPCR analysis revealed that transfection with Adv-MEG3 evidently upregulated MEG3 RNA level in M2-type BMDMs (Figure 3A). Then, IL4/IL13-induced M2-type BMDMs were simultaneously transfected with Adv-MEG3. As shown by flow cytometric analysis, overexpressing MEG3 significantly reduced $CD206^{+}$ cell percentage (Figure 3B and C). Furthermore, we also examined M2 polarization marker genes. Consistent with the results of flow cytometry, ARG1, YM1 and MRC1 mRNA levels in M2-type BMDMs were obviously attenuated after MEG3 overexpression (Figure 3D–F). Taken together, MEG3 hindered M2 macrophage polarization.

MEG3 Inhibits M2 Macrophage Polarization-Induced HCC Cell Metastasis and Angiogenesis

Next, we explored whether the function of macrophage on tumor development can be impacted after overexpressing MEG3. BMDMs were treated with IL4/IL13, followed by Adv-MEG3 transfection. Then, cells were cultured with serum-free medium and the supernatants were harvested as conditioned medium (CM). Huh7 cells were incubated with the above CM and the influence of M2-type macrophages on HCC cell migration and invasion was evaluated by Transwell assays. CM collected from M2-type BMDMs increased the numbers of both migrated and invaded Huh7 cells, which, however, were reduced after MEG3 overexpression (Figure 4A–D). Moreover, tube formation experiment demonstrated that the number of luminal formations was increased after culture with CM from M2-type BMDMs, while such increase was reversed after incubation with CM from Adv-MEG3-transfected M2-type BMDMs (Figure 4E and F). In conclusion, MEG3 mitigated HCC cell metastasis and angiogenesis through suppressing M2 macrophage polarization.

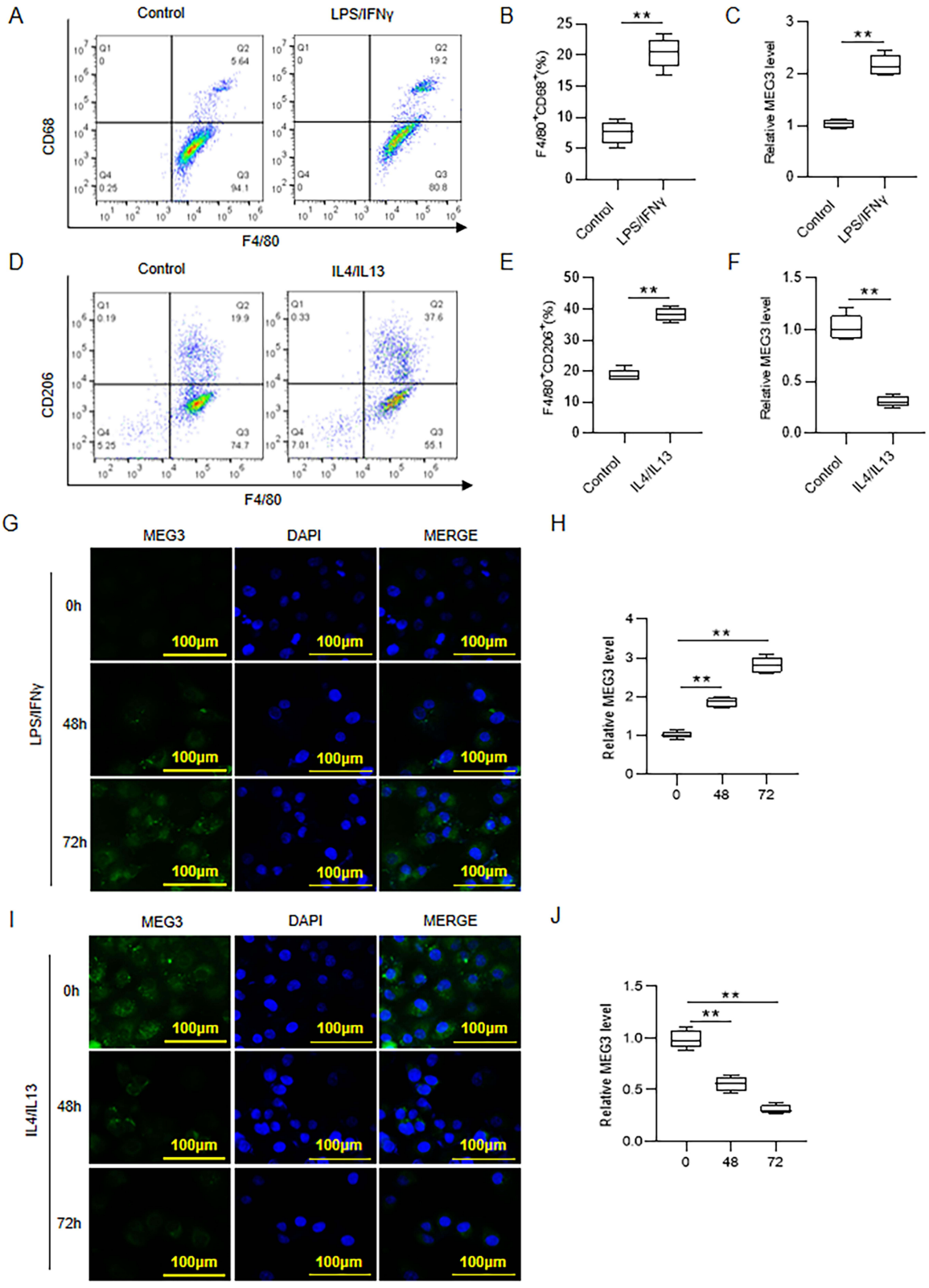

Figure 2 MEG3 participates in M1/M2 macrophage polarization. (**A** and **B**) Analysis of F4/80$^+$CD68$^+$ cell percentage in control and LPS/IFNγ-treated BMDMs by using flow cytometry. (**C**) Detection of MEG3 RNA level in BMDMs after LPS/IFNγ treatment by RT-qPCR. (**D** and **E**) Analysis of F4/80$^+$CD206$^+$ cell percentage in control and IL4/IL13-treated BMDMs through flow cytometry. (**F**) Evaluation of MEG3 RNA level in BMDMs after IL4/IL13 treatment by RT-qPCR. (**G** and **H**) Assessment of MEG3 expression in BMDMs after 0, 48 or 72 h treatment of LPS/IFNγ by FISH assay and RT-qPCR analysis. (**I** and **J**) Determination of MEG3 expression in BMDMs after 0, 48 or 72 h treatment of IL4/IL13 by FISH assay and RT-qPCR analysis. **p < 0.01.

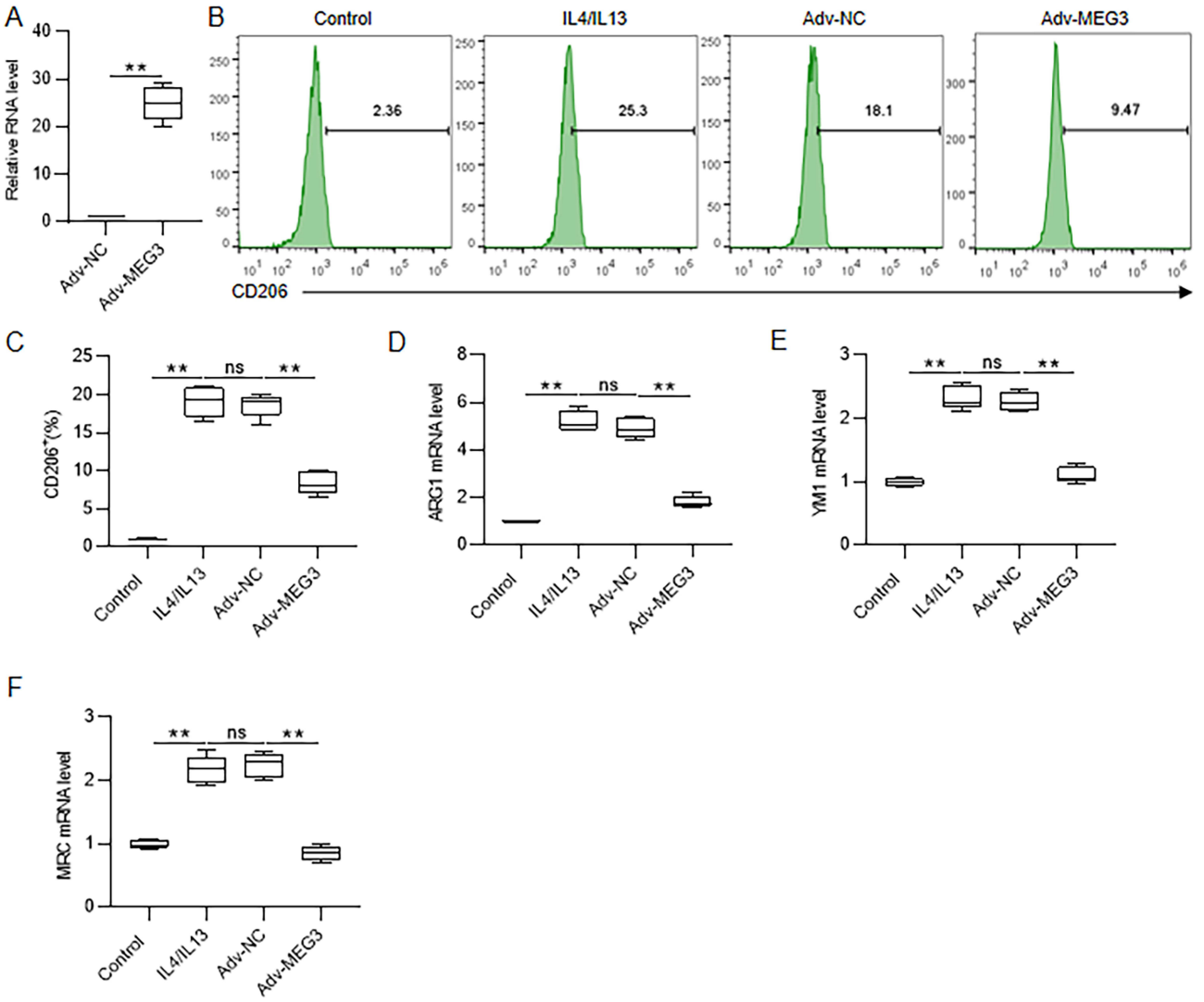

Figure 3 MEG3 suppressed M2 macrophage polarization. (**A**) Adenovirus vector overexpressing MEG3 (Adv-MEG3) and control vector (Adv-NC) were transfected into IL4/IL13-induced M2-type BMDMs, and the overexpression efficiency was confirmed by RT-qPCR. (**B** and **C**) BMDMs were treated with IL4/IL13 to induced M2 phenotype and simultaneously transfected with Adv-NC or Adv-MEG3. $CD206^+$ cell percentage was determined through flow cytometric analysis. (**D**–**F**) Assessment of mRNA levels of M2 macrophage marker genes in M2-type BMDMs after Adv-MEG3 or Adv-NC transfection by RT-qPCR. **p < 0.01.

MEG3 Represses in vivo Tumor Growth by Curbing M2 Macrophage Polarization

To assess the in vivo therapeutic effects of MEG3, the mixture of Huh7 cells and Adv-NC or Adv-MEG3-transfected M2-type BMDMs were implanted subcutaneously into the armpits of nude mice. We found that the primary tumors excised from mice implanted with Huh7 cells and Adv-NC-transfected M2-type BMDMs were prominently bigger than those excised from mice implanted with Huh7 cells only but were smaller than those obtained from mice implanted with Huh7 cells and Adv-MEG3-transfected M2-type BMDMs (Figure 5A). What is more, MEG3 overexpression in M2-type BMDMs markedly reduced tumor weight, but did not affect body weight (Figure 5B and C). As revealed by H&E staining, overexpressing MEG3 considerably ameliorated the histopathological changes of tumors stimulated by M2-type BMDMs in nude mouse xenograft model (Figure 5D). Immunohistochemistry staining indicated that tumor tissues from mice injected with MEG3-overexpressed cell mixture displayed decreased levels of Ki67 and CD206 (Figure 5E–H). The expression of M2 polarization markers was also downregulated in tumor tissues of mice injected with MEG3-overexpressed cell mixture (Figure 5I–K). Collectively, overexpressing MEG3 in tumor-associated macrophages suppressed M2 macrophage polarization and curbed tumor growth.

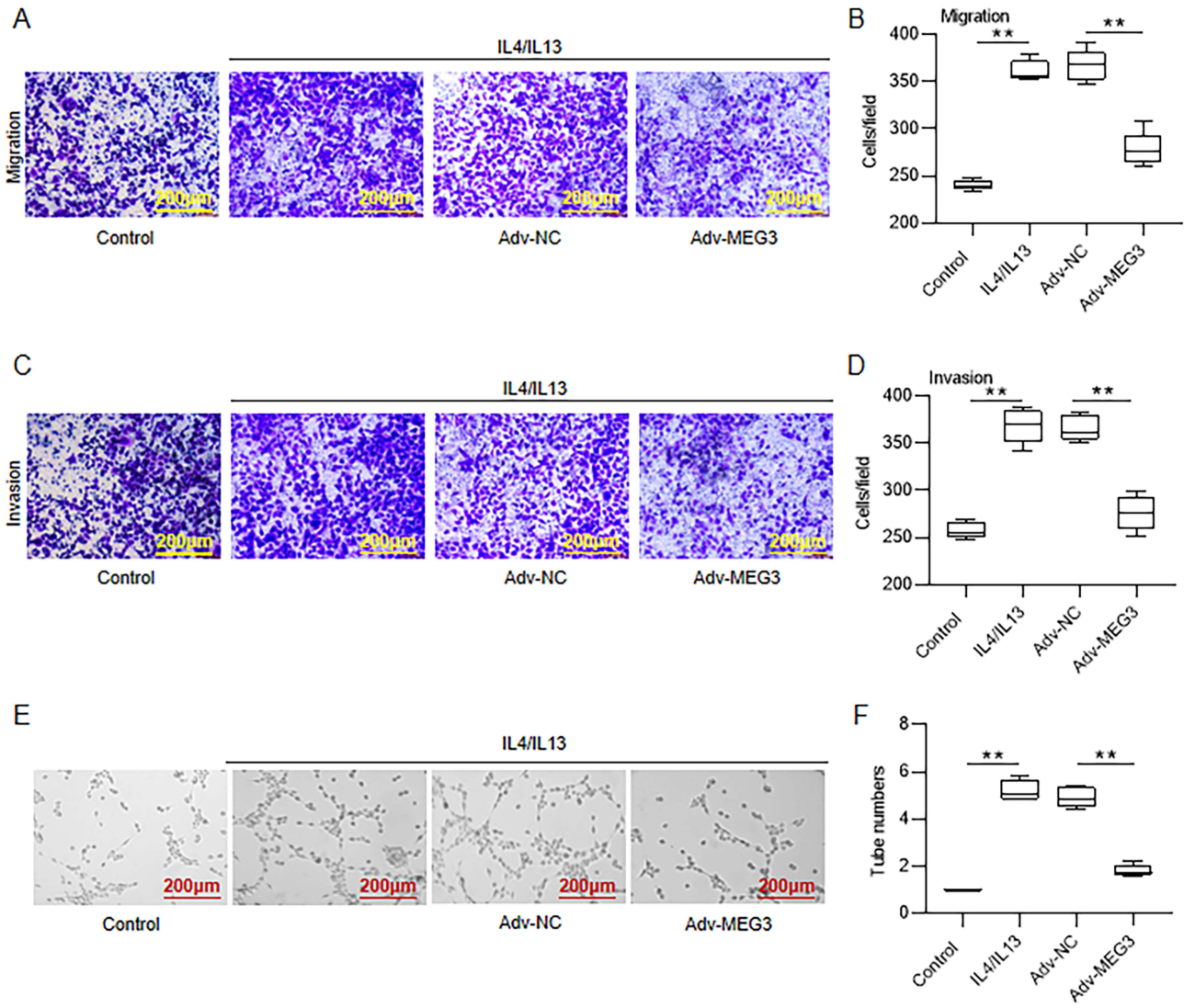

Figure 4 MEG3 inhibits M2 macrophage polarization-induced HCC cell metastasis and angiogenesis. Huh7 cells were cultured for 24 h with condition medium (CM) from Adv-MEG3-transfected M2-type BMDMs. (**A**–**D**) Examination of Huh7 cell migration and invasion by Transwell assays. (**E** and **F**) Measurement of capillary-like tube formation of HUVECs in the presence of CM through tube formation experiment. **p < 0.01.

LncRNA MEG3 Binds with miR-145-5p

LncRNAs exert their biological roles in tumor development through various mechanisms, one of which is the ceRNA regulatory mechanism. LncRNAs competitively bind with the corresponding miRNAs and thereby regulate the expression of downstream target mRNAs. Therefore, we hypothesized that lncRNA MEG3 may also serve as a ceRNA in modulating HCC development. Under the screening condition of clipExpNum>5, five candidate miRNAs harboring MEG3 binding sites were predicted at ENCORI database (Table 1). Huh7 cells were transfected with Adv-NC or Adv-MEG3 to examine the changes in the mRNA levels of the above five miRNAs in response to MEG3 overexpression. The findings of RT-qPCR illustrated that only miR-145-5p mRNA level was obviously reduced in MEG3-overexpressed Huh7 cells (Figure 6A), which help us identify the promising role of miR-145-5p in MEG3-mediated HCC development. Besides, miR-145-5p expression was dramatically attenuated in LPS/IFNγ-induced M1-type BMDMs, but was substantially enhanced in IL4/IL13-induced M2-type BMDMs (Figure 6B and C), suggesting the potential involvement of miR-145-5p in M1/M2 macrophage polarization. Then, Huh7 cells were transfected with miR-NC or miR-145-5p mimics, and the overexpression efficiency was confirmed by RT-qPCR. Compared with miR-NC, miR-145-5p mimics caused a notable increase in miR-145-5p expression in Huh7 cells (Figure 6D). According to ENCORI database, the binding

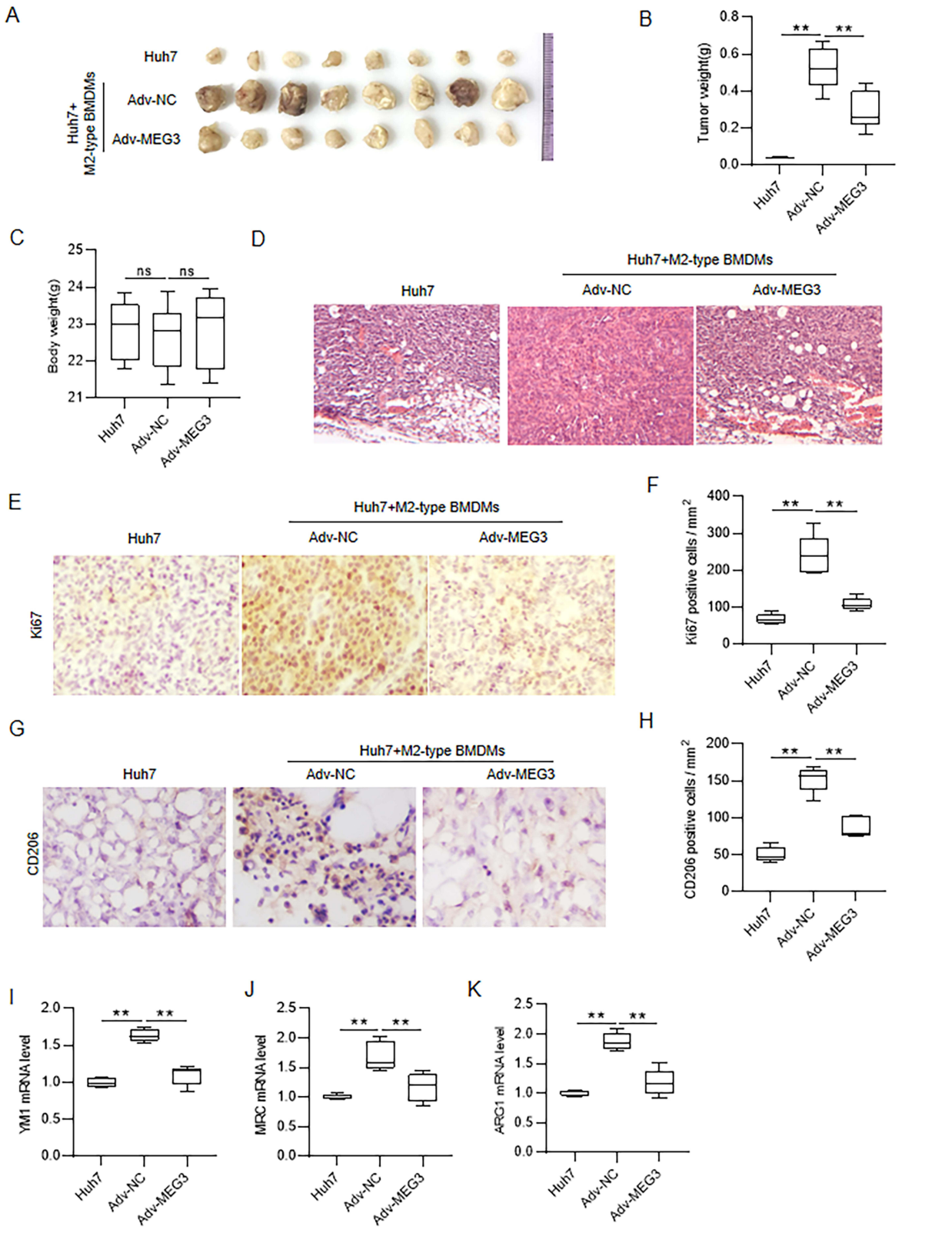

Figure 5 MEG3 represses in vivo tumor growth by inhibiting M2 macrophage polarization. Nude mice were injected subcutaneously with Huh7 cells only, mixture of Huh7 cells and Adv-NC-transfected M2-type BMDMs, or mixture of Huh7 cells and Adv-MEG3-transfected M2-type BMDMs. (**A**) The primary tumors were excised and photographed after mice were sacrificed. (**B**) Tumor weight. (**C**) Body weight of mice. (**D**) Examination of the histopathological characteristics of the tumors by hematoxylin and eosin (H&E) staining. (**E**–**H**) Determination of Ki67 and CD206 expression in tumor tissues by immunohistochemistry staining. (**I**–**K**) Detection of mRNA expression of M2 polarization markers by RT-qPCR analysis. N = 8 per group. **p < 0.01.

Table 1 Five Candidate Downstream miRNAs of MEG3 Predicted at ENCORI Database (Screening Condition: clipExpNum>5)

miRNAid	miRNAname	geneID	geneName	geneType	clipExpNum
MIMAT0000437	hsa-miR-145-5p	ENSG00000214548	MEG3	lincRNA	8
MIMAT0021127	hsa-miR-5195-3p	ENSG00000214548	MEG3	lincRNA	8
MIMAT0015023	hsa-miR-3150a-3p	ENSG00000214548	MEG3	lincRNA	8
MIMAT0027426	hsa-miR-6763-5p	ENSG00000214548	MEG3	lincRNA	8
MIMAT0019700	hsa-miR-4640-3p	ENSG00000214548	MEG3	lincRNA	8

sites of miR-145-5p on MEG3 were shown (Figure 6E). To verify the binding of miR-145-5p on MEG3, luciferase reporter assays were conducted. We discovered that overexpressing miR-145-5p attenuated the luciferase activity of pmirGLO vector containing wild-type MEG3 but not mutant MEG3 (Figure 6F). Altogether, lncRNA MEG3 might mediate macrophage phenotypic polarization in HCC development through sponging miR-145-5p.

MiR-145-5p Direct Targets DAB2

According to miRDB database, seven candidate target genes of miR-145-5p were screened out under the condition of target score = 100 (Figure 7A). After overexpressing miR-145-5p in Huh7 cells, we discovered that DAB2 expression was notably downregulated while other candidate genes showed no significant change in their expression (Figure 7B). Thus, DAB2 was selected for our following assays. Similarly, we also detected the expression of DAB2 in the process of M1/M2 macrophage polarization. DAB2 expression was upregulated in LPS/IFNγ-induced M1-type BMDMs, but was downregulated in IL4/IL13-induced M2-type BMDMs (Figure 7C and D). TargetScan database showed that miR-145-5p bound with DAB2 3'UTR at position 1084–1091 and 1604–1610 (Figure 7E). A luciferase reporter assay was then conducted to verify the relationship between miR-145-5p and DAS2. Overexpressing miR-145-5p caused a marked

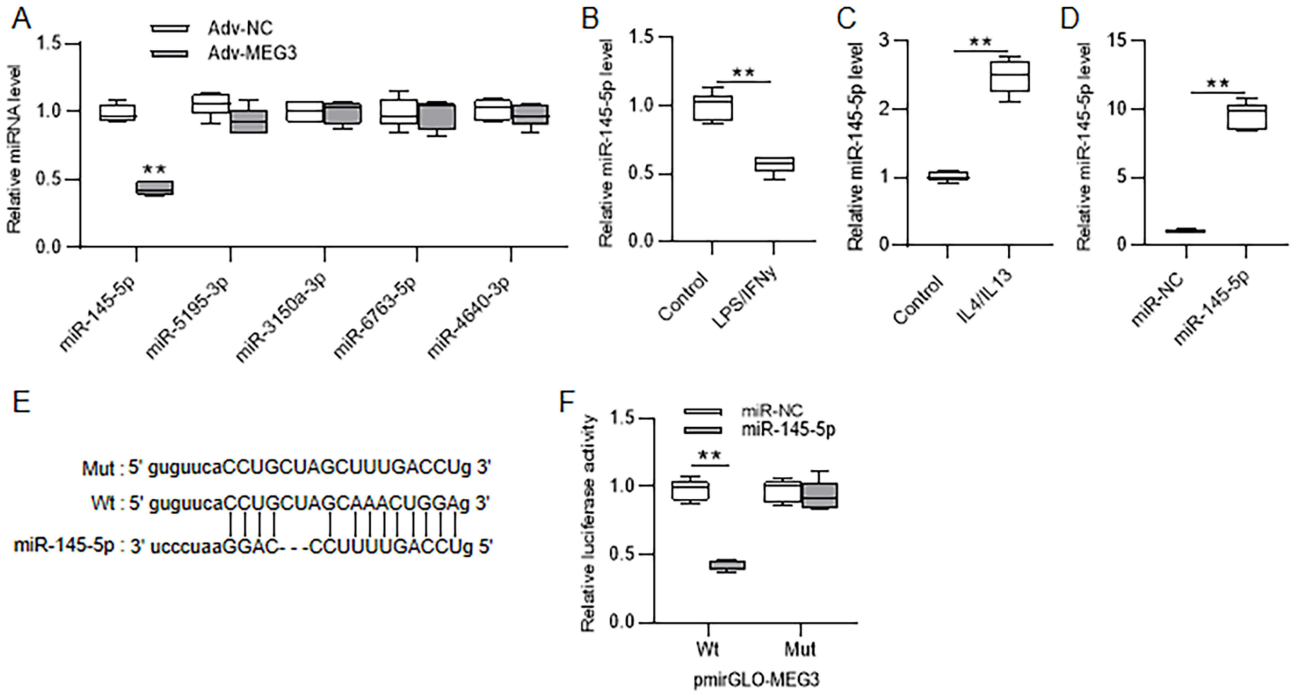

Figure 6 LncRNA MEG3 binds with miR-145-5p. (**A**) Evaluation of the mRNA levels of five candidate downstream miRNAs of MEG3 in Huh7 cells transfected with Adv-NC or Adv-MEG3 by RT-qPCR. (**B** and **C**) Detection of miR-145-5p expression level in LPS/IFNγ-induced M1-type and IL4/IL13-induced M2-type BMDMs by RT-qPCR. (**D**) Examination of miR-145-5p expression in Huh7 cells transfected with miR-NC or miR-145-5p by RT-qPCR. (**E**) The binding site of miR-145-5p on MEG3 shown at ENCORI database (https://starbase.sysu.edu.cn/). (**F**) Huh7 cells were cotransfected with pmirGLO vectors carrying wild-type or mutant binding site of MEG3 and miR-NC or miR-145-5p mimics. The luciferase activities of vectors were measured after 48 h. **p < 0.01.

A

Target Detail	Target Rank	Target Score	miRNA Name	Gene Symbol	Gene Description
Details	1	100	hsa-miR-145-5p	FSCN1	fascin actin-bundling protein 1
Details	2	100	hsa-miR-145-5p	ABHD17C	abhydrolase domain containing 17C
Details	3	100	hsa-miR-145-5p	FLI1	Fli-1 proto-oncogene, ETS transcription factor
Details	4	100	hsa-miR-145-5p	MRTFB	myocardin related transcription factor B
Details	5	100	hsa-miR-145-5p	DAB2	DAB2, clathrin adaptor protein
Details	6	100	hsa-miR-145-5p	SRGAP1	SLIT-ROBO Rho GTPase activating protein 1
Details	7	100	hsa-miR-145-5p	SRGAP2	SLIT-ROBO Rho GTPase activating protein 2

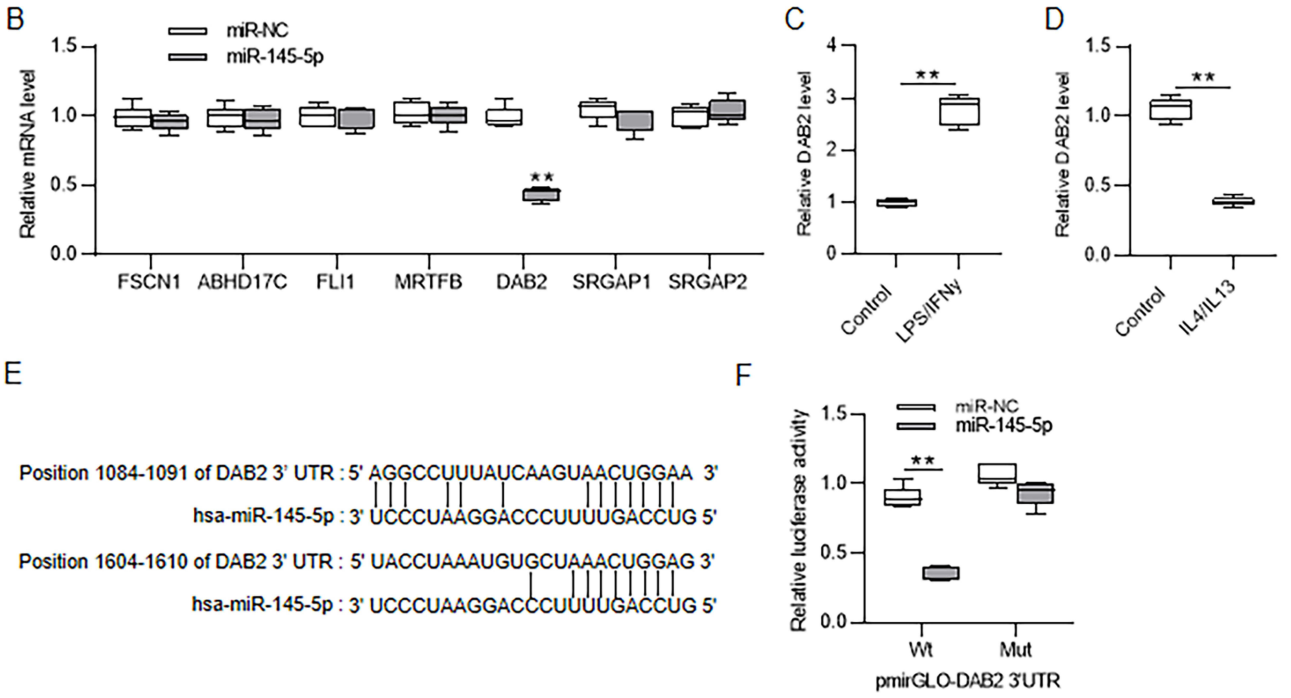

Figure 7 MiR-145-5p direct targets DAB2. (**A**) Prediction of candidate target genes of miR-145-5p at miRDB database (https://mirdb.org/) under the screening condition of target score=100. (**B**) Analysis of changes in candidate gene expression after miR-145-5p overexpression in Huh7 cells by RT-qPCR. (**C** and **D**) Assessment of DAB2 expression level in LPS/IFNγ-induced M1-type and IL4/IL13-induced M2-type BMDMs by RT-qPCR. (**E**) The binding sites of miR-145-5p on DAB2 3'UTR predicted at TargetScan database (https://www.targetscan.org/). (**F**) Huh7 cells were cotransfected with pmirGLO vector containing wild-type or mutant fragment of DAB2 3'UTR and miR-NC or miR-145-5p mimics. The luciferase activities were detected 48 h later. **p < 0.01.

reduction in the luciferase activity of pmirGLO vector containing wild-type 3'UTR of DAB2 but not mutant 3'UTR of DAB2 (Figure 7F). In summary, DAB2 was a downstream target of miR-145-5p.

DAB2 Knockdown Reverses the Influence of MEG3 Overexpression on HCC Cell Metastasis and Angiogenesis

Finally, to confirm whether MEG3 mediates HCC development through modulating M2 macrophage polarization via targeting DAB2, rescue experiments were carried out. Huh7 cells were transfected with adenovirus vector delivering shDAB2 (Adv-shDAB2), which led to a substantial reduction in DAB2 mRNA and protein expression (Figure 8A–C). IL4/IL13-induced M2-type BMDMs were transfected with Adv-MEG3 and Adv-shDAB2. Then, conditioned medium (CM) was collected as mentioned above. Huh7 cells were incubated with CM for 24 h, followed by Transwell assays of cell migration and invasion. The findings demonstrated that incubation with CM collected from Adv-MEG3-transfected M2-type BMDMs significantly decreased M2-type macrophage-induced migration and invasion of Huh7 cells. In contrast, DAB2 silencing counteracted the suppression of MEG3 overexpression on Huh7 cell migratory and invasive abilities (Figure 8D–G). Besides, co-transfection with

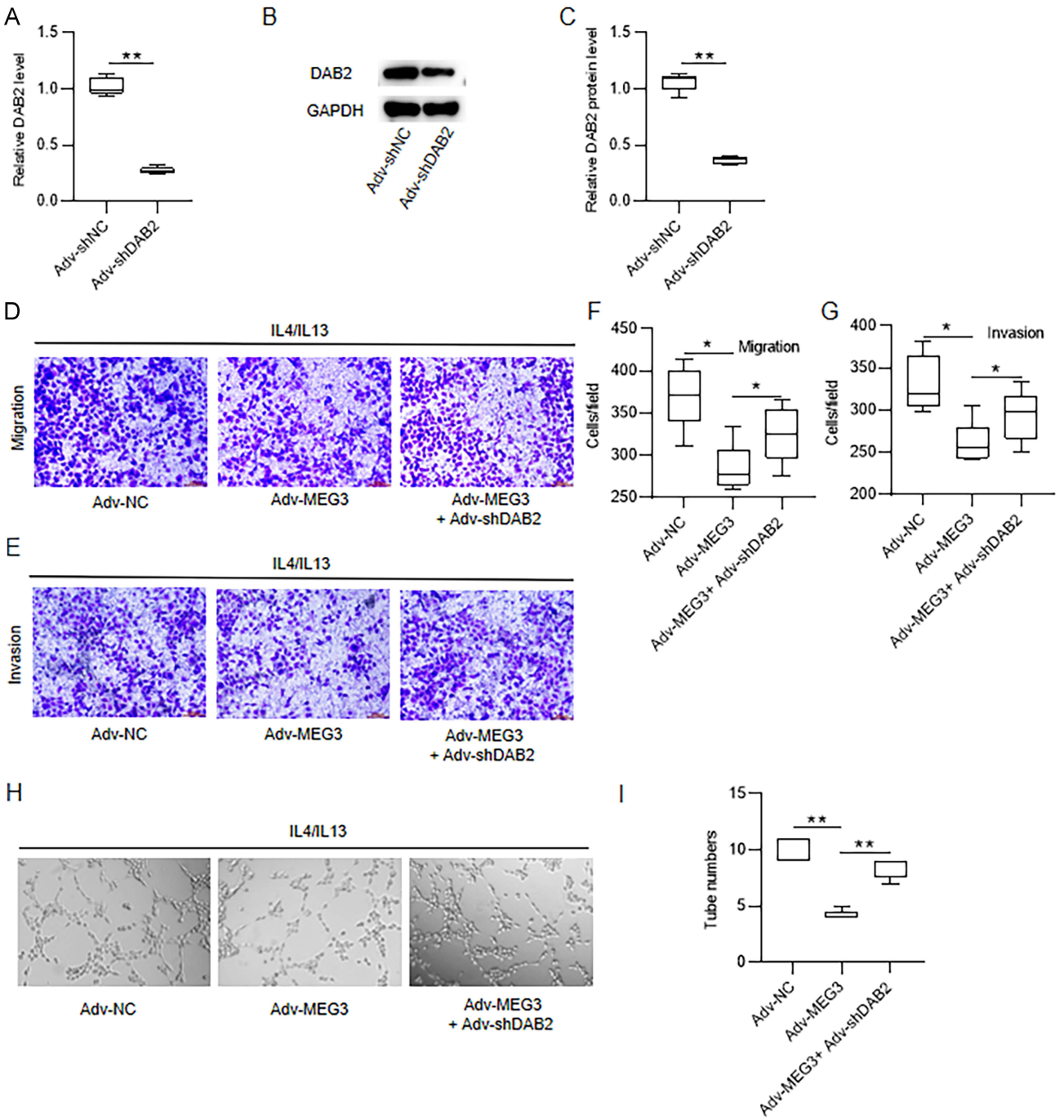

Figure 8 DAB2 knockdown reverses the influence of MEG3 overexpression on HCC cell metastasis and angiogenesis. (**A**–**C**) Huh7 cells were transfected with Adv-shNC or Adv-shDAB2, and the interfering efficiency of DAB2 was determined by RT-qPCR and Western blotting. (**D**–**G**) Huh7 cells were cultured for 24 h with condition medium (CM) from Adv-MEG3+Adv-shDAB2-cotransfected M2-type BMDMs. Huh7 cell migratory and invasive abilities were examined via Transwell assays. (**H** and **I**) Tube-like structures formation of HUVECs in vitro was measured through endothelial cell tube formation assay. *$p < 0.05$, **$p < 0.01$.

Adv-MEG3 and Adv-shDAB2 antagonized the inhibitory effects of Adv-MEG3 transfection alone on the tube formation capability of Huh7 cells (Figure 8H and I). Therefore, MEG3 repressed M2 macrophage polarization-induced HCC cell metastasis and angiogenesis by upregulating DAB2.

Discussion

Cancer metastasis and recurrence have always been the major factors that contribute to the low survival rates of HCC patients.[35] Emerging evidence has pointed out that lncRNAs are involved in the regulation of tumor metastasis in various

human malignancies, including HCC.[36] In our study, we discovered that overexpressing lncRNA MEG3 evidently repressed M2 macrophage polarization in BMDMs and subsequently attenuated the metastasis and angiogenesis of HCC cells. Mechanically, MEG3 bound with miR-145-5p and affected DAB2 expression.

TME is the main battlefield of the competition between the tumor and the host immune system.[37] The interaction between various cells in the TME causes immune cells to have a dual role dependent on the TME and determines the outcome of the tumor-associated immune response – ie, the immune system's attack or tolerance to tumor cells.[38] The formation of TME during cancer development promotes tumor cell growth and metastasis.[39] TAMs, as key immune effector cells in the TME, can be recruited to cancer tissues to release chemokines, cytokines, and inflammatory mediators, which play essential role in tumor progression.[40] In TME, macrophages can be converted into two subtypes, M1-type and M2-type macrophages.[41] M1-type macrophages are responsible for pro-inflammatory cytokine production and secretion, which are always activated by Th1 cytokines LPS and IFN-γ. M1-type macrophages phagocytose and destroy microorganisms, remove tumor cells, and present antigens to T cells to elicit adaptive immune responses.[42] In comparison, M2-like polarized macrophages play an anti-inflammatory function and usually participate in regulating angiogenesis, wound healing, and tissue remodeling, which are often activated by Th1 cytokines IL4 and IL13.[43] Many studies have illuminated that M2 macrophage polarization directly triggers HCC cell growth and metastasis and some lncRNAs have been demonstrated to influence HCC cell malignant behaviors through mediating M2 macrophage polarization. For example, Wang et al disclosed that lncRNA DLX6-AS1 enhanced HCC cell epithelial-mesenchymal transition, migration and invasion through inducing M2 macrophage polarization by sponging miR-15a-5p to upregulate CXCL17 expression.[44] Tian et al discovered that lncRNA LINC00662 repressed HCC cell apoptosis but facilitated HCC cell growth, cell cycle, invasion via activating Wnt/β-catenin pathway and M2 macrophage polarization.[45] Wang et al reported that lncRNA HMMR-AS1 prevented ARID3A degradation by competitively bind to miR-147a, which significantly promoted the M2 polarization of macrophages and thereby accelerate HCC progression.[46] In our research, we discovered that MEG3 expression was enhanced during LPS/IFNγ-induced M1 polarization but was reduced during IL4/IL13-induced M2 polarization, implying the participation of MEG3 in macrophage polarization during the development of HCC. Furthermore, MEG3 overexpression obviously repressed M2 macrophage polarization in vitro, as evidenced by decreased levels of CD206-positive cells and reduced expression of the M2 polarization markers ARG1, YM1 and MRC1. The results of in vivo experiments showed that tumor tissues obtained from mice injected with MEG3-overexpressed cell mixture displayed decreased expression of CD206 and M2 polarization markers.

Since M2 macrophage phenotypic polarization is closely related to tumor cell malignant phenotypes, we then evaluated whether MEG3 overexpression influences M2 macrophage polarization-induced HCC cell metastasis and angiogenesis. Although the relationship between MEG3 and macrophage polarization in HCC was not explored before, the role of MEG3 in HCC development has been extensively elucidated. As mentioned in the previous study, MEG3 expression was markedly lower in serum samples and tumor tissues from HCC patients than in healthy controls, and MEG3 knockdown promoted HCC cell growth and metastasis through increasing TGF-β1 expression.[47] Importantly, lncRNA MEG3 exert its biological effects in HCC development through the ceRNA regulatory mechanism. For instance, Zhang et al clarified that MEG3 bound with miRNA-10a-5p and upregulated PTEN expression, thus attenuating the growth and metastasis of proliferation of HCC cell line HepG2 but boosting the apoptosis and cell cycle arrest at G1 stage.[31] Liu et al demonstrated that overexpressing MEG3 facilitated cell apoptosis but curbed cell growth in HCC via modulating the miR-9-5p/SOX11 axis.[48] Li et al disclosed that MEG3 suppressed HCC cell viability and migration and restrained HCC progression in a xenograft tumor model by modulating the miR-5195-3p/FOXO1 signaling axis.[49] In our research, the findings revealed that the migratory, invasive and tube formation capabilities of Huh7 cells were substantially weakened after co-culture with condition medium harvested from MEG3-overexpressed M2-type BMDMs, suggesting the repression of MEG3 on M2 macrophage polarization-induced HCC cell metastasis and angiogenesis.

Based on the above literature, our study also used bioinformatic tools to predict the downstream miRNAs of MEG3 to confirm its ceRNA network. MiR-145-5p was discovered as a candidate miRNA of MEG3, and their binding was further validated by luciferase reporter assay. Overexpression of MEG3 led to a remarkable reduction in miR-145-5p expression. Previously, numerous studies have demonstrated that miR-145-5p plays a tumor suppressive role in human cancers such

as renal cancer, cholangiocarcinoma, cervical cancer, breast cancer and bladder cancer,[50] while few studies have reported its oncogenic role in tumorigenesis. Interestingly, miR-145-5p was found to be downregulated in HCC tissues and cell lines, and miR-145-5p induced apoptosis but suppressed cell proliferation, migration, and invasion in HCCLM3 cells by targeting ARF6.[51] Similarly, Gu et al[52] and Dong et al[53] also verified that miR-145-5p functioned as a tumor suppressor in HCC. However, our study showed that miR-145-5p was negatively regulated by MEG3, and miR-145-5p expression was downregulated after M1 macrophage polarization but upregulated after M2 macrophage polarization. Therefore, miR-145-5p might play an oncogenic role in HCC development. The reason for the dual effects of miR-145-5p in HCC might depend on the functions of different target genes. MiRNAs regulate posttranscriptional gene expression through binding to the 3'UTR target mRNAs. Herein, DAB2 was identified as a direct target of miR-145-5p. DAB2, as a multifunctional scaffold protein expressed abundantly in human platelets, is involved in cell growth, homeostasis, differentiation, cell–cell interactions, and platelet aggregation.[54] Previous research has illustrated that DAB2 is downregulated in metastatic bladder cancer, prostate cancer and colorectal cancer.[55–57] Moreover, Wang et al discovered that DAB2 interfered with the Wnt and Hippo signaling pathways, thereby repressing gastric cancer migration.[58] Herein, DAB2 depletion circumvented the inhibition of MEG3 overexpression on HCC cell migration, invasion and angiogenesis, indicating that MEG3 hindered HCC development by upregulating DAB2.

Collectively, our study confirmed that lncRNA MEG3 suppressed cell metastasis and angiogenesis in HCC through the M2 macrophage polarization. The mechanism through which MEG3 exerted its biological role in HCC was also determined. MEG3 curbed HCC progression via sponging miR-145-5p and increasing DAB2 expression. Our results might provide a novel direction for identifying MEG3 as a therapeutic target for HCC.

Data Sharing Statement

The datasets used during the current study are available from the corresponding author on reasonable request.

Funding

The work was supported by Guangxi Science and Technology Project (Grant no.2021AC20006), and High-level personnel project of Affiliated Hospital of Youjiang Medical University for Nationalities (Grant no. R202210307).

Disclosure

The authors declare no conflicts of interest in this work.

References

1. Sung H, Ferlay J, Siegel RL, et al. Global cancer statistics 2020: GLOBOCAN estimates of incidence and mortality worldwide for 36 cancers in 185 countries. *CA Cancer J Clin*. 2021;71(3):209–249. doi:10.3322/caac.21660
2. Cai Y, Lyu T, Li H, et al. LncRNA CEBPA-DT promotes liver cancer metastasis through DDR2/β-catenin activation via interacting with hnRNPC. *J Exp Clin Cancer Res*. 2022;41(1):335. doi:10.1186/s13046-022-02544-6
3. Marrero JA, Fontana RJ, Fu S, et al. Alcohol, tobacco and obesity are synergistic risk factors for hepatocellular carcinoma. *J Hepatol*. 2005;42 (2):218–224. doi:10.1016/j.jhep.2004.10.005
4. Yang JD, Hainaut P, Gores GJ, et al. A global view of hepatocellular carcinoma: trends, risk, prevention and management. *Nat Rev Gastroenterol Hepatol*. 2019;16(10):589–604. doi:10.1038/s41575-019-0186-y
5. Grandhi MS, Kim AK, Ronnekleiv-Kelly SM, et al. Hepatocellular carcinoma: from diagnosis to treatment. *Surg Oncol*. 2016;25(2):74–85. doi:10.1016/j.suronc.2016.03.002
6. Lurje I, Czigany Z, Bednarsch J, et al. Treatment strategies for hepatocellular carcinoma ‑ a multidisciplinary approach. *Int J Mol Sci*. 2019;20 (6):1465. doi:10.3390/ijms20061465
7. Finn RS, Zhu AX, Farah W, et al. Therapies for advanced stage hepatocellular carcinoma with macrovascular invasion or metastatic disease: a systematic review and meta-analysis. *Hepatology*. 2018;67(1):422–435. doi:10.1002/hep.29486
8. Junttila MR, de Sauvage FJ. Influence of tumour micro-environment heterogeneity on therapeutic response. *Nature*. 2013;501(7467):346–354. doi:10.1038/nature12626
9. Xiao Y, Yu D. Tumor microenvironment as a therapeutic target in cancer. *Pharmacol Ther*. 2021;221:107753. doi:10.1016/j.pharmthera.2020.107753
10. Coussens LM, Zitvogel L, Palucka AK. Neutralizing tumor-promoting chronic inflammation: a magic bullet? *Science*. 2013;339(6117):286–291. doi:10.1126/science.1232227
11. Wang Y-C, He F, Feng F, et al. Notch signaling determines the M1 versus M2 polarization of macrophages in antitumor immune responses. *Cancer Res*. 2010;70(12):4840–4849. doi:10.1158/0008-5472.CAN-10-0269

12. Zhou D, Luan J, Huang C, et al. Tumor-associated macrophages in hepatocellular carcinoma: friend or foe? *Gut Liver*. 2021;15(4):500–516. doi:10.5009/gnl20223
13. Wang Y, Gao R, Li J, et al. Downregulation of hsa_circ_0074854 suppresses the migration and invasion in hepatocellular carcinoma via interacting with HuR and via suppressing exosomes-mediated macrophage M2 polarization. *Int J Nanomedicine*. 2021;16:2803–2818. doi:10.2147/IJN.S284560
14. Yin Z, Ma T, Lin Y, et al. Retracted: IL-6/STAT3 pathway intermediates M1/M2 macrophage polarization during the development of hepatocellular carcinoma. *J Cell Biochem*. 2018;119(11):9419–9432. doi:10.1002/jcb.27259
15. Klichinsky M, Ruella M, Shestova O, et al. Human chimeric antigen receptor macrophages for cancer immunotherapy. *Nat Biotechnol*. 2020;38(8):947–953. doi:10.1038/s41587-020-0462-y
16. Qiu Y, Chen T, Hu R, et al. Next frontier in tumor immunotherapy: macrophage-mediated immune evasion. *Biomark Res*. 2021;9(1):72. doi:10.1186/s40364-021-00327-3
17. Wang L, Cho KB, Li Y, et al. Long noncoding RNA (lncRNA)-mediated competing endogenous RNA networks provide novel potential biomarkers and therapeutic targets for colorectal cancer. *Int J Mol Sci*. 2019;20(22):5758.
18. Tan Y-T, Lin J-F, Li T, et al. LncRNA-mediated posttranslational modifications and reprogramming of energy metabolism in cancer. *Cancer Commun*. 2021;41(2):109–120. doi:10.1002/cac2.12108
19. Chan JJ, Tay Y. Noncoding RNA: RNA regulatory networks in cancer. *Int J Mol Sci*. 2018;19(5):1310. doi:10.3390/ijms19051310
20. Chen L, Qiu C-H, Chen Y, et al. LncRNA SNHG16 drives proliferation, migration, and invasion of lung cancer cell through modulation of miR-520/VEGF axis. *Eur Rev Med Pharmacol Sci*. 2020;24(18):9522–9531. doi:10.26355/eurrev_202009_23037
21. Fang Y, Fullwood MJ. Roles, functions, and mechanisms of long non-coding RNAs in cancer. *Genomics Proteomics Bioinformatics*. 2016;14(1):42–54. doi:10.1016/j.gpb.2015.09.006
22. Zhang L, Tao H, Li J, et al. Comprehensive analysis of the competing endogenous circRNA-lncRNA-miRNA-mRNA network and identification of a novel potential biomarker for hepatocellular carcinoma. *Aging*. 2021;13(12):15990–16008. doi:10.18632/aging.203056
23. Teng F, Zhang J-X, Chang Q-M, et al. LncRNA MYLK-AS1 facilitates tumor progression and angiogenesis by targeting miR-424-5p/E2F7 axis and activating VEGFR-2 signaling pathway in hepatocellular carcinoma. *J Exp Clin Cancer Res*. 2020;39(1):235. doi:10.1186/s13046-020-01739-z
24. Wang Y, Yang L, Chen T, et al. A novel lncRNA MCM3AP-AS1 promotes the growth of hepatocellular carcinoma by targeting miR-194-5p/FOXA1 axis. *Mol Cancer*. 2019;18(1):28. doi:10.1186/s12943-019-0957-7
25. Xu J, Wang X, Zhu C, et al. A review of current evidence about lncRNA MEG3: a tumor suppressor in multiple cancers. *Front Cell Dev Biol*. 2022;10:997633. doi:10.3389/fcell.2022.997633
26. Du Y, Geng G, Zhao C, et al. LncRNA MEG3 promotes cisplatin sensitivity of cervical cancer cells by regulating the miR-21/PTEN axis. *BMC Cancer*. 2022;22(1):1145. doi:10.1186/s12885-022-10188-0
27. Wei GH, Wang X. lncRNA MEG3 inhibit proliferation and metastasis of gastric cancer via p53 signaling pathway. *Eur Rev Med Pharmacol Sci*. 2017;21(17):3850–3856.
28. Wu M, Huang Y, Chen T, et al. LncRNA MEG3 inhibits the progression of prostate cancer by modulating miR-9-5p/ QKI-5 axis. *J Cell Mol Med*. 2019;23(1):29–38. doi:10.1111/jcmm.13658
29. Yang Z, Wang Z, Duan Y. LncRNA MEG3 inhibits non-small cell lung cancer via interaction with DKC1 protein. *Oncol Lett*. 2020;20(3):2183–2190. doi:10.3892/ol.2020.11770
30. Sun K-X, Wu -D-D, Chen S, et al. LncRNA MEG3 inhibit endometrial carcinoma tumorigenesis and progression through PI3K pathway. *Apoptosis*. 2017;22(12):1543–1552. doi:10.1007/s10495-017-1426-7
31. Zhang Y, Liu J, Lv Y, et al. LncRNA meg3 suppresses hepatocellular carcinoma in vitro and vivo studies. *Am J Transl Res*. 2019;11(7):4089–4099.
32. Toda G, Yamauchi T, Kadowaki T, et al. Preparation and culture of bone marrow-derived macrophages from mice for functional analysis. *STAR Protoc*. 2021;2(1):100246. doi:10.1016/j.xpro.2020.100246
33. Weischenfeldt J, Porse B. Bone Marrow-Derived Macrophages (BMM): isolation and applications. *CSH Protoc*. 2008;2008:pdb.prot5080. doi:10.1101/pdb.prot5080
34. Zong S, Dai W, Guo X, et al. LncRNA-SNHG1 promotes macrophage M2-like polarization and contributes to breast cancer growth and metastasis. *Aging*. 2021;13(19):23169–23181. doi:10.18632/aging.203609
35. Zhou C, Liu C, Liu W, et al. SLFN11 inhibits hepatocellular carcinoma tumorigenesis and metastasis by targeting RPS4X via mTOR pathway. *Theranostics*. 2020;10(10):4627–4643. doi:10.7150/thno.42869
36. Dong J, Teng F, Guo W, et al. lncRNA SNHG8 promotes the tumorigenesis and metastasis by sponging miR-149-5p and predicts tumor recurrence in hepatocellular carcinoma. *Cell Physiol Biochem*. 2018;51(5):2262–2274. doi:10.1159/000495871
37. Oura K, Morishita A, Tani J, et al. Tumor immune microenvironment and immunosuppressive therapy in hepatocellular carcinoma: a review. *Int J Mol Sci*. 2021;22(11):5801. doi:10.3390/ijms22115801
38. Guizhen Z, Guanchang J, Liwen L, et al. The tumor microenvironment of hepatocellular carcinoma and its targeting strategy by CAR-T cell immunotherapy. *Front Endocrinol*. 2022;13:918869. doi:10.3389/fendo.2022.918869
39. Sas Z, Cendrowicz E, Weinhäuser I, et al. Tumor microenvironment of hepatocellular carcinoma: challenges and opportunities for new treatment options. *Int J Mol Sci*. 2022;23(7):3778. doi:10.3390/ijms23073778
40. Wang H, Yung MM, Ngan HY, Chan KK, Chan DW. The impact of the tumor microenvironment on macrophage polarization in cancer metastatic progression. *Int J Mol Sci*. 2021;22(12):6560.
41. Boutilier AJ, Elsawa SF. Macrophage polarization states in the tumor microenvironment. *Int J Mol Sci*. 2021;22(13):6995. doi:10.3390/ijms22136995
42. Min L, Wang H, Qi H. Astragaloside IV inhibits the progression of liver cancer by modulating macrophage polarization through the TLR4/NF-κB/STAT3 signaling pathway. *Am J Transl Res*. 2022;14(3):1551–1566.
43. Liu H, Wang M, Jin Z, et al. FNDC5 induces M2 macrophage polarization and promotes hepatocellular carcinoma cell growth by affecting the PPARγ/NF-κB/NLRP3 pathway. *Biochem Biophys Res Commun*. 2021;582:77–85. doi:10.1016/j.bbrc.2021.10.041
44. Wang LP, Lin J, Ma X-Q, et al. Exosomal DLX6-AS1 from hepatocellular carcinoma cells induces M2 macrophage polarization to promote migration and invasion in hepatocellular carcinoma through microRNA-15a-5p/CXCL17 axis. *J Exp Clin Cancer Res*. 2021;40(1):177. doi:10.1186/s13046-021-01973-z

45. Tian X, Wu Y, Yang Y, et al. Long noncoding RNA LINC00662 promotes M2 macrophage polarization and hepatocellular carcinoma progression via activating Wnt/β-catenin signaling. *Mol Oncol*. 2020;14(2):462–483. doi:10.1002/1878-0261.12606
46. Wang X, Zhou Y, Dong K, et al. Exosomal lncRNA HMMR-AS1 mediates macrophage polarization through miR −147a/ ARID3A axis under hypoxia and affects the progression of hepatocellular carcinoma. *Environ Toxicol*. 2022;37(6):1357–1372. doi:10.1002/tox.23489
47. Dong H, Zhang Y, Xu Y, et al. Downregulation of long non-coding RNA MEG3 promotes proliferation, migration, and invasion of human hepatocellular carcinoma cells by upregulating TGF-β1. *Acta Biochim Biophys Sin*. 2019;51(6):645–652. doi:10.1093/abbs/gmz046
48. Liu Z, Chen JY, Zhong Y, et al. lncRNA MEG3 inhibits the growth of hepatocellular carcinoma cells by sponging miR-9-5p to upregulate SOX11. *Braz J Med Biol Res*. 2019;52(10):e8631. doi:10.1590/1414-431x20198631
49. Li M, Liao H, Wu J, et al. Long noncoding RNA matrilineal expression gene 3 inhibits hepatocellular carcinoma progression by targeting microRNA-5195-3p and regulating the expression of forkhead box O1. *Bioengineered*. 2021;12(2):12880–12890. doi:10.1080/21655979.2021.2005986
50. Kadkhoda S, Ghafouri-Fard S. Function of miRNA-145-5p in the pathogenesis of human disorders. *Pathol Res Pract*. 2022;231:153780. doi:10.1016/j.prp.2022.153780
51. Wang S, Wang T, Gu P. microRNA-145-5p inhibits migration, invasion, and metastasis in hepatocellular carcinoma by inhibiting ARF6. *Cancer Manag Res*. 2021;13:3473–3484. doi:10.2147/CMAR.S300678
52. Gu X, Zhang J, Ran Y, et al. Circular RNA hsa_circ_101555 promotes hepatocellular carcinoma cell proliferation and migration by sponging miR-145-5p and regulating CDCA3 expression. *Cell Death Dis*. 2021;12(4):356. doi:10.1038/s41419-021-03626-7
53. Dong G, Zhang S, Shen S, et al. SPATS2, negatively regulated by miR-145-5p, promotes hepatocellular carcinoma progression through regulating cell cycle. *Cell Death Dis*. 2020;11(10):837. doi:10.1038/s41419-020-03039-y
54. Tsai H-J, Huang C-L, Chang Y-W, et al. Disabled-2 is required for efficient hemostasis and platelet activation by thrombin in mice. *Arterioscler Thromb Vasc Biol*. 2014;34(11):2404–2412. doi:10.1161/ATVBAHA.114.302602
55. Karam JA, Shariat SF, Huang H-Y, et al. Decreased DOC-2/DAB2 expression in urothelial carcinoma of the bladder. *Clin Cancer Res*. 2007;13(15 Pt 1):4400–4406. doi:10.1158/1078-0432.CCR-07-0287
56. Rosenbauer F, Kallies A, Scheller M, et al. Disabled-2 is transcriptionally regulated by ICSBP and augments macrophage spreading and adhesion. *EMBO J*. 2002;21(3):211–220. doi:10.1093/emboj/21.3.211
57. Zhou J, Scholes J, Hsieh JT. Characterization of a novel negative regulator (DOC-2/DAB2) of c-Src in normal prostatic epithelium and cancer. *J Biol Chem*. 2003;278(9):6936–6941. doi:10.1074/jbc.M210628200
58. Wang H, Dong S, Liu Y, et al. DAB2 suppresses gastric cancer migration by regulating the Wnt/β-catenin and Hippo-YAP signaling pathways. *Transl Cancer Res*. 2020;9(2):1174–1184. doi:10.21037/tcr.2019.12.96